Study of the derived based catalysts from *Theobroma cacao* pod husks for the conversion of Beef Tallow blend with Waste used vegetable oil for fatty acid ethyl ester synthesis: Burnt, Submerged fermented, Calcination, Hybrid Design, Catalyst refining and reusability

Adepoju TUNDE FOLORUNSHO (avogadros2002@yahoo.com)
Akwa Ibom State University https://orcid.org/0000-0002-0782-3996
Ibeh A Mayen
Akwa Ibom State University
Babatunde E O
University of Ilorin
Asuquo A Jackson
Akwa Ibom State University
Eloboka C
Northwest University

Research

Keywords: Catalysts, Biomass wastes, Calcination, Recycle, Reused, Fatty acid ethyl ester

Posted Date: July 17th, 2020

DOI: https://doi.org/10.21203/rs.3.rs-39335/v1

Abstract

Billions of dollars paid by industries on catalysts used as feedstocks to obtain their end products are increasing at a geometrical rate, the report revealed that the global market size was estimated at USD 26.1 billion in 2019 and is expected to reach USD 34.0 billion in 2025. To salvage the world from extravagance spending, there is an urgent need for biomass wastes consideration and utilization. In this paper, three novel CaO-based catalysts derived from *Theobroma cacao* pod husks were tested based on efficacy for the synthesis of fatty acid ethyl ester (FAEE) from the blend of beef tallow-waste use oil in the ratio of 5:95 (BTO_5),10:90 (BTO_{10}),15:85 (BTO_{15}), 20:80 (BTO_{20}),....., 95:5 (BTO_{95}), respectively. Process optimization of the transesterification reaction was carried out using a hybrid design to determine the effects of catalyst on the FAEE yield. The efficiencies of the catalyst were tested via the refining and reusability test. Results revealed the oil blend ratio of BTO_{60}: WUO_{40} sufficiently produced low viscous oil that was easily converted to biodiesel. Catalysts' characterization revealed the three catalysts produced high CaO-based of 68.20, 81.46, and 87.65 (wt.%), which accounted for the high yield of FAEEs. Mathematical optimization showed that the catalyst amount (F-value between 14159.69-3063.24 with P-value between 0.0053–0.0115), played the most significant role in oil conversion to biodiesel among the constraint factors considered (reaction time, catalyst amount, reaction temperature, and EtOH/OMR). Based on Box-Cox transformation, the values of the lambda obtained indicated a normal data results with an inverse function of Y^2 and Y^3 and normal function of Y^3 for polynomial model accuracy. Optimum validated FAEEs yields of 92.81, 93.02, and 99.64 (%wt.), respectively, with high R^2. The qualities of the FAEEs were within the standard specification and the produced catalysts can serve as feedstocks for industrial application.

1.0 Introduction

Many chemical reactions involved the use of one or more catalysts for reaction to reach completion. The type of catalyst used in a particular reaction depends solely on the reaction conditions and the nature of reactants involved. Although catalysts are not to be consumed in the reaction, its presence speeds up or limits reaction rate, and itself recover at the end of product formation. Nowadays, industries such as pharmaceuticals, polymers, petroleum, electronic, environmental treatment, chemical, and agrochemical industries employ the use of catalysts to achieve the end products. Also, the use of catalysts occupies an important place in academic research. A recent report revealed that the worldwide market value of catalysts was estimated in 2019 at USD 26.1 billion, and is expected to reach USD 27.2 billion in 2020, and USD 34.0 billion in 2025 at growth rate 4.5% according to Compound Annual Growth Rate (CAGR). This makes it a value-added income for the financial sustainability of all nations if biomass waste can be employed. However, catalysts are primarily divided into four categories; homogeneous catalyst, heterogeneous catalyst, heterogenized-homogeneous catalysis, and biocatalysts.

Homogeneous catalysis involved the operation of the mixture in the same phase, the possible reactant and the catalyst exhibit a high uniform phase due to high reactivity and selectivity. Most oxidation, carbonylation, hydrogenation, esterification, and hydrocyanation are homogeneous catalysis in reaction. However, this nature of catalyst usage comes with its shortcoming, this includes recoverability problem, highly toxic, and high cost, especially in esterification (bio-fuel production) case.

Heterogeneous catalysis, on the other hand, involved the mixture that exists in different phases; the catalyst usually solid support or bulk form does not dissolve in the reactant, yet exhibit high reactivity. The advantages include ease of recoverability and reused, non-toxic, and of low cost. These have made many industries such as hydrocarbon produced company (Fischer process), ammonia synthesis company (Haber-Bocsch process), sulphuric acid company (Contact process), soap making company (Saponification process), and petroleum company (transesterification process) to adhere to the use of this catalysts, apart from these advantages, heterogeneous catalysts produce in smaller particle size increase its activity due to surface phenomenon. The smaller the particles size the larger the surface area of catalysts during the reaction.

Heterogenized-homogeneous catalysis is the mixture of the heterogeneous and homogeneous catalysts together. The homogeneous catalyst is embedded onto the solid supports to prepare the heterogenic analogy. However, these types of catalysts are difficult to produce due to complexity, less selectivity, reactivity, and covalent bonding between the polymer chain and the surface atoms (grafting).

Biocatalysts are usually referred to as enzymes or ribozymes catalysts obtained from plants, microbes, or Goat tissue, which are used to catalyst reaction that takes place outside the living cells. This type of catalyst is on high industrial usage and has been considered an alternative to most industrial conventional catalysts due to the advantages such as mild reaction conditions, high selectivity, high efficiency, and non-toxic. Companies such as, dairy, baking, detergent, leather, textile, and biofuel utilized this catalyst for their production. Its major drawbacks are in-ability to convert a cellular catalyst into a bioprocess, difficulty in recoverability (brewing process) sustainability in harsh environmental conditions during culture (high temperature, extreme pH, high salt concentrations, organic solvent), instability in aqueous media (protein), cofactor dependability (non-protein chemical compound), possibility of an allergic reaction, and inactivation through inhibition (Dizge *et al*., 2009)[1].

Among these catalysts, a heterogeneous catalyst is a solid catalyst of calcium-based compound usually prepared from solid wastes and employed as a catalyst for transesterification of oil to biodiesel due to the above-mentioned advantages (Milan *et al*., 2016)[2]. Biodiesel is a renewable, eco-friendly, non-toxic, and sustainable alternative fuel derived from the synthesis of vegetable oil or fat. In the past and also present, reports on solid based developed from solid wastes as heterogeneous catalysts and applied it to the synthesis of biodiesel from vegetable oil. Vadery *et al.* (2014)[3] synthesized biodiesel from *Jatropha* oil through methanolysis of a developed based catalyst from coconut husk ash, while Bazargan *et al.* (2015) [4] adopted the used of palm kernel shell gasification as a heterogeneous catalyst for biodiesel production. Chouhan *et al.* (2013)[5] converted *Jatropha curcus* oil to biodiesel through the help of *Lemna perpusila* Torrey ash, but, Razaei *et al.* (2013) [6]used waste mussel shell as a catalyst to synthesized biodiesel. The work of Ikbal *et al.* (2018) [7] reported the use of waste snail shells as a heterogeneous catalyst for the production of biodiesel from soybean oil, while in 2019, Subramaniapillai [8] and co used *Donax delltoides* shell as heterogeneous catalyst. The use of pearl spar as a heterogeneous catalyst was employed in the study reported by Adepoju *et al*. (2018)[9], while in another work, Betiku *et al*. (2015)[10] developed heterogeneous catalyst from plantain peel, applied it to biodiesel synthesis from yellow oleander. The study conducted in another work by Betiku *et al*. (2017)[11] reported the use of heterogeneous catalyst developed from cocoa pod husks, while

Nath *et al.* (2019)[12] developed heterogeneous catalyst from waste *Brassica nigra* plant for biodiesel production. In the work of Balajii *et al.* (2020)[13], the heterogeneous catalyst was made from the Banana peduncle, meanwhile, Minakshi *et al.* (2020)[14] used *Carica papaya* stem as a bio-based catalyst. Further study by Hadiyanto *et al.* (2016)[15] utilized *Anadara granosa* as a heterogeneous CaO-based catalyst, but, Trisupakitti *et al.* (2019) [16] used golden apple cherry snail as a heterogeneous catalyst to synthesized biodiesel from the vegetable. Falowo *et* al. (2020)[17] developed a novel mesoporous base catalyst synthesis from a mixture of three agro-wastes. All these reports developed catalysts from mixture or single solid wastes, and applied it to the synthesis of biodiesel from vegetable oil or its blend, except in the work of Adepoju, (2020) [18] where two derived base catalysts were tested on the synthesized biodiesel from the blended oil.

Therefore, to cover the gap between the efficiency of the developed catalysts derived from single or the mixture of solid wastes, and to introduce a novel blend ratio through the BTO5, BTO10, BTO15,……., BTO95 in an interval of 5 between the Beef Tallow Oil (BTO) and Waste Used Vegetable Oil (WUVO) for process industry (bio-fuel or margarine), this study developed three CaO-based catalysts from a burnt *Theobroma cacao* pod husk (BTCPH), calcined *Theobroma cacao* pod husk (CTCPH), and submerged fermented calcined *Theobroma cacao* pod husk (SFCTCPH), applied each for the synthesis of biodiesel from the blended of the oil obtained from Beef tallow-vegetable used oil. The catalysts prepared were characterized using Scanning Electron Microscopy (SEM), Energy Dispersive Spectroscopy (EDS), X-ray diffraction analysis (XRD), Fourier transforms infrared spectroscopy (FTIR), and BET adsorption analysis. Process modeling and optimization of biodiesel synthesis was carried out by considering five levels-four factors (reaction time, reaction temperature, catalyst amount, and ethanol to oil molar ratio (EtOH/OMR)) via Box Behnken Experimental Design (BBED). Catalysts regeneration and reusability were carried out, and the suitability of the biodiesel in an internal combustion engine was established by determining the physicochemical properties.

2. Materials And Methods

2.1 Materials

WUVO was obtained from a local restaurant, in Eket, beef tallow was obtained from an abattoir in Mkpat Enin L.G.A, Akwa Ibom State, Nigeria. The WUVO was heated in an opened container at 100 ^{o}C on a hot plate for 30 min, allowed to cool to room temperature, and then filtered to remove dirt. The cleaned oil was then stored in a covered jar for further processing. The collected beef tallow was washed in a container with 500 ml of Na_2CO_3 (1 mol/l) and stirred for 30 min mechanically. The mixture was centrifuged at 3500 rpm for 10 min at a temperature of 25 ^{o}C using a propylene tube. The supernatant was separated by filtration, and 40 g of anhydrous Na_2SO_4 was added, stirred for 8 min, and was centrifuged again for 6 min at a temperature of 25 ^{o}C (Adepoju, 2020)[18]. The pure beef tallow oil (PBTO) obtained was kept in a clean covered jar for further use.

Cocoa pod husk was collected from a local Cocoa processing village in Ondo State. The pod husk was washed with distilled water trice and allowed to be free of water at room temperature for 24 h. After 24 h, the washed pod husks free of water was divided into three-samples: Sample A was burnt in the open air until its completely formed ash; the ash was separated into smaller particle sizes (0.30 mm) by sieving, labelled as BTCPH. Sample B was milled into powder, separated into a smaller particle size of 0.3 mm by mesh sieve, and then calcined at 750 ^{o}C for 4 h in a furnace. Sample C was fermented in distilled water anaerobically (submerged) for 10 days, and then the fermented sample was separated from fermented water by decantation, dried in an oven at 120 ^{o}C until a constant weight was achieved (bone dried). The dried fermented sample was milled and sieved into powder of 0.33 mm particle size before calcined at 750 ^{o}C for 4 h in a furnace. Both samples B (CTCPH) and C (SFCTCPH) after calcination were left in the furnace for 24 h for proper cooling, and then placed in cleaned containers as well as BTCPH for further characterization to determine their potential as a heterogeneous catalyst for industrial application (biofuel production).

All chemicals used in this study were of analytical graded and need no further purifications, and were supplied by Sigma Aldrich.

2.2 Catalysts calcination and characterization

Samples BTCPH, CTCPH, and SFCTCPH were characterized by SEM to study the surface morphology of the samples, XRD equipped with Kά and Cu radiation source, accelerated at 20 mA and 40 kV, to establish the angular scanning electron performed in the range of $10^{o} < 2\theta < 80^{o}$ at speed of 2.5 ^{o}C min^{-1} and to verify the elemental analysis of the samples and the quantitative composition of the samples. FTIR was used to confirm the presence of functional group and verify the presence of characteristic absorption bands of major elements present within the crystals powder structures. The pore volume, surface area, basic density site, and the total basic density were examined using BET isothermal adsorption and Hammett indicator.

2.3 Oil blend and its physicochemical properties

For proper oil mixed, it is necessary to know the synergy behind the oil mixed, a probability guesses mixed adopted in reported studies might result in fuel-engine problems. The key factors to be considered in mixing oil are the oil low viscosity, high volatility, and moderate acid value. Since there is no single report on the blend/mix ratio of BTO and WUVO, therefore this study adopted the following blend/mix ratios for BTO:WUVO in volumetric ratios as; 5:95 (BTO_5),10:90 (BTO_{10}),15:85 (BTO_{15}), 20:80 (BTO_{20}), 25:75 (BTO_{25}), 30:70 (BTO_{30}), 35:65 (BTO_{35}), 40:60 (BTO_{40}), 45:55 (BTO_{45}),50:50 (BTO_{50}),55:45 (BTO_{55}), 60:40 (BTO_{60}), 65:35 (BTO_{65}), 70:30 (BTO_{70}), 75:35 (BTO_{75}), 80:20 (BTO_{80}), 85:15 (BTO_{85})„ 90:10 (BTO_{90}), 95:5 (BTO_{95}), respectively. These ratios were chosen to ascertain oil with low viscous, high volatility, and low acid value that enhanced higher biodiesel yield using the derived CaO-based heterogeneous catalysts. 5:95 (BTO_5) is an abbreviation for 5 ml of BTO and 95 ml of WUVO.

The blended oil in different ratios was properly mixed by heating at 35 ^{o}C on a hot plate for easy miscibility considering the instability in fat nature. Each resulting mixture was examined for its viscosity, the acid value, and the specific gravity. The mixture with low acid value, low specific gravity, and low viscosity was used for biodiesel synthesis. Other properties of the blended oil were further determined using the association of official analytical chemists (AOAC 1997

2.4. Biodiesel production

Production of biodiesel was carried out through the ethanolysis of CaO-based catalyst derived from the samples. The reaction process take placed in a 1000 ml capacity-three-necked-reactor, 200 ml of the blended oil was first preheated on a hot plate with a magnetic stirrer for 60 min at 100 ^{o}C. 2.5 (wt.) of CaO catalyst was measured in a 250 ml dried-cleaned flask, and 50 ml of ethanol was measured and added to the ethanol flask to achieved EtOH/OMR of 1:4. The mixture was placed on a shaker for 15 min and then added to the preheated oil on the hot plate. Two layers were observed, the ethanol-catalyst layer, and the oil layer, the stirrer was inserted, and the reaction was monitored at 70 ^{o}C for 65 min.

At the reaction completion, the insoluble catalyst was separated through decantation, and the remained product (ethanol-biodiesel) was distinguished through gravity in a separating funnel. The obtained fatty acid ethyl ester (biodiesel) contained adherent catalyst (leached catalyst), which was removed by washing with hot methanolic sodium carbonate (1.0 g $NaCO_3$ dissolved in 20 ml methanol), and was well stirred. The washed mixture was filtered, and the filtrate-diesel was washed with distilled water twice before water-diesel separation through gravity settling. The water wet-diesel was dried over anhydrous sodium sulphate (Na_2SO_4), before separation by decantation to obtain pure biodiesel (fatty acid ethyl ester: FAEE). The residual residue filtered catalyst was collected for reused but was firstly purified. This process was conducted based on the number of experimental designs.

2.5. Experimental design for FAEE

Experimental design software such as Box Behnken Design (BBD), Central Composite Design (CCD), Factorial Design (FD), as well as Tanquchi design (TD) contains a lack of fits in the model analysis. Lack of fits only exist when the experimental design is poor, a poor model of the data, or poor choice of variables. This then results in high residual/error value, experimental replications, and a high number of experimental runs (between 28–45 runs) when considering four-variable-five level-factors. Therefore, to avoid these problems, considering four factors (reaction time, catalyst amount, reaction temperature, and ethanol/oil molar ratio (EtOH/OMR)), a Hybrid Design (HD) with a minimal point design for 3, 4, 6, and 7 factors with 5 level levels each was employed. This design has no replication to avoid time wastage; it has no lack of fits because the residual or error values are so small (10^{-10}) due to better experimental design, and a low number of experimental runs (four factors produced 16 runs) to avoid repetitions. These rotatable designs are better than BBD, CCD, FD, and TD, but are highly sensitive to outlier (missing data). Table 1 displayed the four- five level- four variable- factors, the units, and the symbol used for the HD design.

Table 1
Five level- four variable- factors experimental for FAEE

Variables	Units	Symbol	Levels				
			-2	-1	0	1	2
Reaction time	(min)	X_1	60	65	70	75	80
Catalyst amount	(wt.%)	X_2	1.5	2.0	2.5	3.0	3.5
Reaction temp.	(^{o}C)	X_3	60	65	70	75	80
EtOH/OMR	(ml/ml)	X_4	4	5	6	7	8

2.6 Optimization analysis of FAEE

The experimental results were used for the process optimization analysis of the FAEE production. The response variable was the FAEE yield, the input variables were the factors at five levels evaluated by mean of fit summary. In the second-order model, the effects of variable significant and preferred terms were appraised by model effects. Analysis of variance (ANOVA) was used to interpret the results while diagnostic was used to estimate the fit of the model, and model transformation, the graphical plots were used to interpret and evaluates the model. The probability value (p-value), the f-value (factor value), the degree of freedom (df), and the variance inflation factor (VIF), respectively, were used for model significance. The regression parameters such as the coefficient of determination: R^2, the predicted coefficient of determination: $R^2_{pred.}$, the adjusted coefficient of determination: $R^2_{adj.}$, and the adequate precision: AdEq. Prec., respectively, were used to confirm the model suitability.

Tri-dimensional space (three-dimensional plots) was used as a geometric setting to express the relationship between three variables (two factors and FAEE yield), while the second-order differential equation that further elucidates the relationship between FAEE yield and the four factors is expressed mathematically as Eq. (1).

$$FAEE\ (\%\,wt.) = \varphi_0 + \sum_{i=1}^{k} \varphi_i X_i + \sum_{i=1}^{k} \varphi_{ii} X_i^2 + \sum_{i<j}^{k} \varphi_{ij} X_i X_j + R \qquad (1)$$

Where FAEE is the response in percentage, ϕ_0 is the intercept, ϕ_i is the linear coefficient, ϕ_{ii} is the interaction coefficient, ϕ_{ij} is the quadratic coefficient terms, X_i, X_j are the four factors and R is the residual error.

2.7 Catalyst purification and reusability

The recovered catalysts were tested for its efficiency by carried out the reusability test but were purified before reused. Purification step was carried out by the method used by Adepoju *et al.* (2020a)[21] with modifications as; the recovered catalyst was first washed with methanol to remove the impurity at the surface of FAEE. The washed catalyst with methanol was centrifuged in an inbuilt heating vacuum centrifuge operated

at 3500 rpm, and separated by decantation. The wet catalyst was oven-dried at 80 ^{o}C for 1 h to be free of methanol and then cooled to room temperature before reused.

2.8 Properties of FAEE

Properties of the FAEE such as density, viscosity, moisture content, mean molecular mass, acid value, Saponification value, iodine value, peroxide value, cetane number, higher heating value, API gravity, and diesel index were determined to ascertain its suitability as a replacement for conventional fuel in an internal combustion engine (I.C. engine), via AOAC, 1997[19]. The results were compared with ASTM D6751[22] and EN 14214 [23] recommended standard.

3. Results And Discussion

3.1. Physicochemical properties of the blended oil

Presented in Table 2 are the results of the physicochemical properties of the blended oil in a different ratio. Observation from the table indicated that the blended oil in the different ratio has the same percentage moisture content of 0.02%, all other blends have different values, except for the BTO_{50} and BTO_{85} having the same viscosity (23.10 mm^2/s), and BTO_{25}, BTO_{30}, and BTO_{75} having the same Saponification value (185.00 mg KOH/g oil).

However, since the major key factor in the selection of any oil is the viscosity and specific gravity of the oil, therefore, the BTO_{60} with the low viscosity of 22.30 mm^2/s and a specific gravity of 0.890 was selected as blended oil for FAEE production. This blended oil produced lighter oil with low acid value and high API gravity (Adepoju, 2020b)[24].

Table 2
Results of physicochemical properties of the oil blend

Blends	**Physicochemical Properties**						
Ratio (BTO: WUVO)	MC (%)	SG	V @ 40 ^{o}C (mm^2/s)	AV (mgKOH/g oil)	SV (mg KOH/g oil)	IV (meq O_2/kg oil)	API g
BTO_5	0.020	0.916	26.00	0.345	194	60.22	22.98
BTO_{10}	0.020	0.914	25.80	0.332	192	60.18	23.31
BTO_{15}	0.020	0.911	25.40	0.310	190	60.10	23.82
BTO_{20}	0.020	0.912	24.90	0.303	189	60.03	23.65
BTO_{25}	0.020	0.908	24.87	0.294	185	60.00	24.34
BTO_{30}	0.020	0.910	24.60	0.296	185	59.86	23.99
BTO_{35}	0.020	0.907	23.60	0.284	184	59.82	24.51
BTO_{40}	0.020	0.905	23.50	0.283	186	59.80	24.85
BTO_{45}	0.020	0.902	23.00	0.280	183	59.83	25.37
BTO_{50}	0.020	0.904	23.10	0.262	185	59.56	25.03
BTO_{55}	0.020	0.903	22.82	0.263	182	59.10	25.20
BTO_{60}	0.020	0.890	22.30	0.249	180	58.88	27.49
BTO_{65}	0.020	0.900	22.45	0.248	184	58.70	25.72
BTO_{70}	0.020	0.902	22.52	0.252	186	58.60	25.37
BTO_{75}	0.020	0.909	22.64	0.263	185	59.92	24.17
BTO_{80}	0.020	0.911	22.86	0.272	188	59.94	23.82
BTO_{85}	0.020	0.915	23.10	0.274	190	59.91	23.14
BTO_{90}	0.020	0.913	22.94	0.276	191	59.70	23.48
BTO_{95}	0.020	0.914	22.96	0.277	191	59.89	23.36
M = Moisture content, SG = Specific gravity, V = Viscosity, AV = Acid value, IV = Iodine value, PV = Peroxide value,							
SV = Saponification value, API g = API gravity							

3.2. Characterization and analysis of catalysts

Microscopy (SEM) analysis

The morphological characteristic of the catalysts was carried out by SEM analysis. Figure 1(a, b, and c) displayed the results of SEM analysis of BTCPH, CTCPH, and SFCTCPH at the same magnification of 500x, but different structural outlook performed in 2θ diffraction with a peak from $20^o < 2\theta < 70^o$ at speed of 2 ^oC/min. The image displayed by BTCPH indicated a highly crystal, cracked, less porous, and non-uniform shape structure whereas. This may be due to the burning process, as thermal burning in the open air, caused fusion and barrier for large surface area. The SEM image of CTCPH showed a uniform, highly porous with aggregated sizes and shape. This observation can be attributed to the surface fermentation process which makes it difficult for microorganisms to maintain homogeneous medium, thereby decreases the mineral content and the surface area of the cocoa pod husk powder. Observation from the morphological structure of SFCTCPH indicated a uniformly distributed structure with smaller sizes and shapes and a high surface area. This could be due to submerged fermentation which involves the growth of the microorganism in a homogeneous medium (inter-particle space and surface area) of the substrate and moisture content. However, it was observed that the release of the CaO from $CaCO_3$ was complete at the calcination temperature of 750 ^oC (Betiku *et al*, 2017)[11].

3.2.2 Fourier-transform infrared spectroscopy (FTIR) analysis

The results of FTIR analysis of the burnt and calcined sample powder catalysts are displayed in Fig. 2(a-c). The spectral showed a sinusoidal waveform at different peaks confirming the effects of heat on the thermal degradation of the catalysts. The vivid descriptions of the wavelengths at different peaks for each catalyst which showed the stretches and the bending vibration of organic-inorganic functional groups present are presented in Table 3. The wavelength bands noticed between 693.3–913.2 cm^{-1} for CTCPH, and the bands between 752.9–913.2 cm^{-1} observed for SFCTCPH, and the wavelength stretches found in BTCPH of 879.7–1043.7 cm^{-1}, specified the presence chlorocarbon (C-Cl), O = C = O bending vibration, nitrogen to carbon bond waging and twisting, and the presence of CO_3^{2-} molecules at a lower temperature. The stretches range between 1036.2–1699.7 cm^{-1} observed in SFCTCPH, and 1032.5–1982.9 cm^{-1} noticed in CTCPH showed similar wavelength due to fermentation process involved, but the value of 1088.4–1379.1 cm^{-1} bands found in BTCPH confirmed the presence of sp^3 of C-C in alkane, sp^2 delocalized electron of C = C in alkene, C = N of imines, and the bending vibration of O-Ca-O in calcium carbonate. Furthermore, 1420.1–1654.3 cm^{-1} wavelength bands noticed in cm^{-1} BTCPH, the value range of 1893.5–2322.1 cm^{-1} observed in the wavelength bands of SFCTCPH, and the range between 1982.9–2050.0 cm^{-1} displayed by CTCPH indicated the presence of C = O of ketone, -CHO of aldehyde, C = C of ester, C-C of alkyne/acetylene, C-N of cyanogen, and O-H of complex molecules. Further observation also indicated the presence of O-H bending structure in alcohol and phenol, O = O of dioxygen, and NO of sp were found in BTCPH, CTCPH, and SFCTCPH at wavelength bands of 1923.3–2974.5 cm^{-1}, 3623.0–3693.8 cm^{-1}, and 3641.6–3753.4 cm^{-1}, respectively, but the long stretches (> 3500) found in CTCPH and SFCTCPH showed the presence of amine and amide bonding structures (Adepoju *et al*., 2020b)[24]. This showed that fermentation increased the presence of functional groups and the surface area of the sample, but the calcined fermented submerge *Theobroma cacao* pod husk SFCTCPH showed more functional groups.

Table 4
FTIR sample spectrum analysis

SN	Wavelength (cm^{-1})	Transmittance (%)	Bonds and Functional groups
BTCPH			
1	879.7 -1043.7	58.079–29.767	C-Cl, CO_3^{2-}, N-H waging and twisting, O = C = O bending vibration
2	1088.4 - 1379.1	29.767–79.771	C-C, C = C, C = N, and O-Ca-O bending vibration
3	1420.1–1923.3	82.562–98.503	C = O, CHO, C ≡ C, C ≡ N, O = C=O of low energy, and O-H
4	2974.5–3336.0	71.078–68.824	O-H bending structure, O = O, and N ≡ O
CTCPH			
1	693.3–913.2	86.990–70.688	C-Cl, C-C. CO_3^{2-}, N-H waging and twisting, O = C = O bending vibration
2	1032.5–1830.1	57.307–97.256	C-C, C = C, C = N, and O-Ca-O bending vibration
3	1982.9–2050.0	96.325–98.896	C = O, CHO, C ≡ C, C ≡ N, and O-H
4	3623.0–3693.8	94.405–98.587	O-H bending structure, O = O, N ≡ O, Amine, and Amide
SFCTCPH			
1	752.9–913.2	83.708–84.559	C-Cl, C-C. CO_3^{2-}, N-H waging and twisting, O = C = O bending vibration
2	1036.2–1699.7	81.649–87.699	C-C, C = C, C = N, and O-Ca-O bending vibration
3	1893.5–2322.1	92.902–90.263	C = O, CHO, C ≡ C, C ≡ N, and O-H
4	3641.6–3753.4	75.796–88.068	O-H bending structure, O = O, N ≡ O, Amine, and Amide

3.2.3 Brunauer-Emmett-Teller (BET) and XRD analysis

Displayed in Table 5 are the results of the analysis of BET and XRD of the catalysts sample. A strong basic site (176, 188, and 196) was found in the catalysts which suggested that the produced catalyst are capable to be used as heterogeneous catalysts for FAEE production, as well as for other industrial applications. The basic site density does not depend on the pore volume of the catalysts but depends solely on the surface area of the catalysts. The higher

the surface area, the lesser the basic site density, hence, the value of 176.00 μmole/m^2 obtained for BTCPH, 170.91 μmole/m^2 obtained for CTCPH, and 178.18 μmole/m^2 obtained for SFCTCPH. The results of XRD analysis showed that the total basic site was responsible for the high conversion of calcium carbonate to calcium oxide. Even, when the burning and calcination temperature was responsible for the formation of CaO with gaseous evolution of CO_2, the reaction is not complete without the process route. Truly, the fermentation process increased the content of CaO obtained in the catalysts, but SFCTCPH has high conversion with 87.65% with a high FAEE yield of 98.94 (% wt.). The yield of FAEE was also high for CTCPH with 94.82 (% wt.), but the value produced by BTCPH was the least with 90.20 (% wt.) due to low CaO conversion of 68.20%. This showed that the calcined fermented catalyst produced higher CaO-based content than the burnt and non-fermented catalysts (Adepoju, 2020)[18].

Table 5
BET and XRD analysis of the catalysts

Catalysts	β (m^2/g)	λ (cm^3/g)	CaO (%)	BS (μmole.g^{-1}) 400 < BS < 650 >650		TBS	BSD (μmole/m^2)	FAEE (%wt.)	CA (wt.%)
BTCPH	1.00	0.0015	68.20	36	140	176	176.00	91.00	2.50
CTCPH	1.10	0.0024	81.46	26	162	188	170.91	94.00	2.50
SFCTCPH	1.10	0.0030	87.65	22	174	196	178.18	98.20	2.50

β = Surface area, λ = Pore volume, BS = Basic site, TBS = Total basic site, BSD = Basic site density, GD = Green diesel, CA = Catalyst amount

3.3. Experimental results and the optimization of transesterification process variables

3.3.1 Experimental results

Displayed in Table 3 are the 16 results obtained for every experimental run carried out and the predicted value by the HD using the three catalysts developed from cocoa pod husk (BTCPH, CTCPH, and CSFCTCPH). Observation from the table showed that FAEE highest yield obtained when BTCPH was used was 93. 50 (%wt.) while the predicted value was 93.50 (%wt.) at run 15, the highest value of FAEE yield obtained by CTCPH in FAEE2 was 94.50 (%wt.) at run 15 with the same predicted value of 94.50 (%wt.). However, the highest FAEE value obtained when CSFCTCPH was used as catalyst was 99.80 (%wt.), but the predicted value was 99.84 (%wt.) at run 10. These values indicated that the three developed catalysts are suitable for FAEE synthesis and can serve as feedstock for based catalyst in industrial application, but the calcined submerge fermented cocoa pod husk powder produced highest FAEE3 yield CSFCTCPH when compared with the yield associated with the use of BTCPH (93.50 (%wt.)) and CTCPH (93.50 (%wt.). Meanwhile, based on experimental and the predicted yield of FAEEs, the plots in Fig. 3(a) showed the relationship between the experimental results and the predicted values by the design software, the identifier of an appropriate exponent (Lambda = 1) to transform data into a normal shape due to residual error was as indicated in Fig. 3(b). Usually, the Lambda values between − 5 and + 5 showed the transformation data has the highest likelihood of normal data. The value of lambda of 0.47 indicated the data obtained in this study were normal and have the function of Y^1 confirming the polynomial model choice accuracy.

Table 3
a: Experimental results and the predicted value

SN	X_1	X_2	X_3	X_4	FAEE1	FAEE2	FAEE3	PFAEE1	PFAEE2	PFAEE3
1	0.000	0.000	0.000	1.732	89.10	90.30	92.30	89.10	90.30	92.30
2	0.000	0.000	0.000	-0.269	90.20	91.40	93.80	90.20	91.40	93.80
3	-1.000	-1.000	-1.000	0.604	88.30	89.50	90.50	88.31	89.53	90.46
4	1.000	-1.000	-1.000	0.604	90.10	91.00	93.00	90.09	90.98	93.04
5	-1.000	1.000	-1.000	0.604	87.90	89.60	91.60	87.89	89.58	91.64
6	1.000	1.000	-1.000	0.604	88.60	89.80	91.70	88.61	89.83	91.66
7	-1.000	-1.000	1.000	0.604	88.60	89.90	90.90	88.59	89.88	90.94
8	1.000	-1.000	1.000	0.604	90.60	92.00	96.24	90.61	92.02	96.20
9	-1.000	1.000	1.000	0.604	91.60	93.90	97.20	91.61	93.92	97.16
10	1.000	1.000	1.000	0.604	92.60	94.90	**99.80**	92.59	94.87	**99.84**
11	1.518	0.000	0.000	-1.050	91.80	93.00	99.40	91.80	93.00	99.40
12	-1.518	0.000	0.000	-1.050	84.50	90.00	93.00	84.50	90.00	93.00
13	0.000	1.518	0.000	-1.050	90.30	92.00	96.00	90.30	92.00	96.00
14	0.000	-1.518	0.000	-1.050	82.50	84.40	86.80	82.50	84.40	86.80
15	0.000	0.000	1.518	-1.050	**93.50**	**95.40**	97.90	**93.50**	**95.40**	97.90
16	0.000	0.000	-1.518	-1.050	80.30	83.20	85.00	80.30	83.20	85.00

3.3.2 Response variable optimization

3.3.2.1 Statistical optimization via ANOVA

Displayed in Table 4b are the results of statistical optimization via ANOVA for the response surface quadratic model and the Fits statistics obtained through the catalytic performance during the transesterification reaction. Observation from the table showed that the Model F-values of 194.16, 159.85, and 263.03 with 14 degree of freedom (df), implied the model were significant with P-values < 0.05, but the model 194.16 with an F-value of 11,095.04 is the most significant model (P-value = 0.0075) compared with model 159.85 with F-value of 2283.63, and model 263.03 with model F-value of 1300.18. The table also displayed the significance of the quadratic model factors, values of "Prob > F" less than 0.05 shows variable terms are significant. In this case, all the model terms were significant except X_1^2 and X_1X_3 when FAEE1 was considered, the non-significant quadratic terms found in FAEE2 production were X_3^2, X_1X_2, X_1X_3, and X_1X_4, while only X_4, X_4^2, and X_1X_4 were found non-significant when the analysis of the significant factors was carried out on FAEE3 production. Based on the results of Fit statistics datasets, the coefficient of determination obtained showed the model's predictions interaction was good (> 98%) with low standard deviations (< 0.20). The values also showed that there is a certainty above 98% that the model generated explained the data variability (Arjun *et al*., 2019)[26]. Meanwhile, the mean values obtained depicted the high accuracy of the data obtained for the variable factors.

Based on the optimization, the statistical model predicted a FAEE1 yield of 93.4998 (%wt.), FAEE2 yield of 95.2411 (%wt.), and FAEE3 yield of 99.8081 (%wt.) at the process variables conditions of 78.58 min, 3. 37 (wt.%), 79.23 ^oC, and 1:6.66 (vol/vol), respectively (Supplementary file). These values were validated by carrying out three experimental runs under the same condition, the average values of fatty acid ethyl ester obtained were 92.8100 (%wt.) for FAEE1, 93.0200 (%wt.) for FAEE2, and 99.6400 (%wt.) for FAEE3, respectively. These values indicated that all catalysts developed were good as feedstock for industrial applications, but fermented catalyst developed catalyst produced the highest biodiesel yield among others.

Source	Sum of Squares			df	Mean Square			F-Value		
	1 2 3				1 2 3			1 2 3		
Model	194.16	159.85	263.03	14	13.87	11.42	18.79	11095.04	2283.63	1300.18
X_1	21.80	6.94	32.54	1	21.80	6.94	32.54	17442.09	1387.81	2251.71
X_2	17.70	23.83	44.26	1	17.70	23.83	44.26	14159.69	4766.88	3063.24
X_3	64.58	68.17	108.11	1	64.58	68.17	108.11	51663.48	13633.9	7481.75
X_4	18.59	5.93	0.56	1	18.59	5.93	0.56	14874.14	1186.82	38.91
X_1^2	0.023	2.61	12.09	1	0.023	2.61	12.09	18.03	521.63	836.54
X_2^2	2.98	3.70	2.80	1	2.98	3.70	2.80	2386.14	740.98	193.46
X_3^2	1.42	0.55	2.62	1	1.42	0.55	2.62	1134.24	110.97	181.25
X_4^2	7.41	3.63	2.20	1	7.41	3.63	2.20	5925.43	726.94	152.05
X_1X_2	0.55	0.72	3.30	1	0.55	0.72	3.30	441.00	144.00	228.54
X_1X_3	0.031	0.25	3.56	1	0.031	0.25	3.56	25.00	49.00	246.67
X_1X_4	8.62	0.44	1.83	1	8.62	0.44	1.83	6898.37	88.17	126.57
X_2X_3	5.95	8.00	12.65	1	5.95	8.00	12.65	4761.00	1600.00	875.46
X_2X_4	13.92	9.25	9.72	1	13.92	9.25	9.72	11136.70	1849.97	672.64
X_3X_4	31.57	20.83	12.68	1	31.57	20.83	12.68	25255.75	4165.73	877.26
Residual	0.00125	0.005	0.014	1	0.00125	0.005	0.014	-	-	-
Cor Total	194.16	159.86	263.04	15	-	-	-	-	-	-
Significance Factors @ p < 0.0500										**Non-Significant Facto**
FAEE1	X_1, X_2, X_3, X_4, X_2^2, X_3^2, X_4^2, X_1X_2, X_1X_4, X_2X_3, X_2X_4, and X_3X_4									X_1^2 and X_1X_3
FAEE2	X_1, X_2, X_3, X_4, X_2^2, X_1^2, X_4^2, X_2X_3, X_2X_4, and X_3X_4									X_3^2, X_1X_2, X_1X_3, and X
FAEE3	X_1, X_2, X_3, X_1^2, X_2^2, X_3^2, X_1X_2, X_1X_3, X_2X_3, X_2X_4, and X_3X_4									X_4, X_4^2, and X_1X_4

Fits statistics

	R-Squared	Adj R-Squared	Pred R-Squared	Adeq Precision	Std. Dev.	Mean
FAEE1	99.99%	99.98%	99.99%	385.597	0.035	88.78
FAEE2	99.99%	99.96%	99.98%	178.192	0.071	90.64
FAEE3	99.98%	99.92%	99.97%	127.523	0.12	93.45

Meanwhile, the second-order mathematical differential equation that correlated the response variables (FAEE1, FAEE2, and FAEE3) with the constraint variables (X_1: reaction time, X_2: catalyst amount, X_3: reaction temperature, and X_4: EtOH/OMR) are presented in Eq. (2), (3), and (4), respectively.

$$\text{FAEE1 (\%wt.)} = +90.61 + 1.32X_1 + 1.18X_2 + 2.26X_3 + 1.21X_4 - 0.26X_1X_2 + 0.063X_1X_3 - 1.04X_1X_4 + 0.86X_2X_3 - 1.32X_2X_4 - 1.99X_3X_4 + 0.061X_1^2 - 0.70X_2^2 - 0.48X_3^2 - 1.21X_4^2 \quad (2)$$

$$\text{FAEE2 (\%wt.)} = +91.65 + 0.74X_1 + 1.37X_2 + 2.33X_3 + 0.69X_4 - 0.30X_1X_2 + 0.17X_1X_3 - 0.23X_1X_4 + 1.00X_2X_3 - 1.08X_2X_4 - 1.61X_3X_4 + 0.65X_1^2 - 0.78X_2^2 - 0.30X_3^2 - 0.85X_4^2 \quad (3)$$

$$\text{FAEE3(\%wt.)} = +93.90 + 1.61X_1 + 1.87X_2 + 2.93X_3 - 0.21X_4 - 0.64X_1X_2 + 0.67X_1X_3 - 0.48X_1X_4 + 1.26X_2X_3 - 1.10X_2X_4 - 1.26X_3X_4 + 1.41X_1^2 - 0.68X_2^2 - 0.65X_3^2 - 0.66X_4^2 \quad (4)$$

Final equation in terms of coded:

The equations showed that the reaction temperature (X_3 with high F-value in Table 4b) and the catalyst amount (X_2 with high F-value) are the most impactful constraint factors on the response yield.

Further mathematical optimization via criteria setting, the constraint variables were set in the ranges, while the responses were set in targets (supplementary file) which produced the graphical interactions between the responses (FAEE1, FAEE2, and FAEE3) and the linear constraint interactions (X_1X_2, X_1X_3, X_1X_4, X_2X_3, X_2X_4, and X_3X_4) known as three-dimensional contour plots are presented in Fig. 4. The plots also proved there were perfect interactions among the variable constraints on the responses. However, the best mutual interactions occurred between X_2X_3 (catalyst amount and reaction temperature), this also showed that catalyst developed as well as reaction temperature played a major role in the conversion of oil to biodiesel. Meanwhile, the least interaction noticed in X_3X_4 (reaction temperature and EtOH/OMR) depicted that the combination of other factors apart from the catalyst produced a low effect. Hence, the effects of the developed catalysts on biodiesel yield are of great important but fermented submerged calcined *Theobroma cocoa* pod husk (FSCTCPH) with coefficient 1.26 in X_2X_3 produced high mutual effects than 1.00 produced by CTCPH and 0.86 observed in BTCPH.

3.4. Catalytic refining and reusability test

Before catalyst reusability, after recycled at the end of the reaction, the catalyst obtained was refined following the step by step procedure of Adepoju *et* al. (2020b)[24] with little modifications. The recovered catalyst was washed with methanol to remove the impurity at the surface of catalyst that occurred during the transesterification, centrifuged at 4500 rpm in an in-built system vacuum centrifuge. The washed catalyst was obtained by filtration, and then oven-dried at 120 ^{o}C for 45 min, cooled to room temperature before reused. The reusability test was carried out on the derived catalysts in many cycles, at the following reaction conditions: the reaction time of 70 min, the catalyst amount of 2.50 (%wt.), the reaction temperature of 70 ^{o}C, and 1:4 (vol/vol) EtOH/OMR. The results obtained were illustrated using Microsoft Excel 2010 to plots the data. The plots showed the activities of the catalysts maintained stability from the first cycle to the 4th cycle with a negligible decrease in catalysts strength, however, a significant dropped was noticed in the 5th and 6th cycles, hence, catalysts refining and reusability were stopped at the 4th cycle. This observation was in line with what was earlier reported that catalyst basic strength decreases due to continuous intermediate products monoglyceride and diglyceride formed during the reaction, which obstructed the catalyst holes. The formation of water to oxygen reaction that occurred at the catalyst surface also reduces the catalyst sensitivity (Trisupakitti *et al*., 2017; Adepoju *et al*., 2020a; Adepoju *et al*., 2020c)[16, 24, 25].

3.5 Fatty acid ethyl ester (FAEEs) qualities and its comparison with standard

Table 5 displayed the results of the qualities of the blended oil (BTO_{60}) and the FAEEs produced with the references to ASTM and EN. Observation from the table indicated that there were significant changes as the oil was converted to biodiesel due to transesterification with developed catalysts, the effect of alcohol, reaction time, and reaction temperature. However, there were no distinct differences in the values of the properties of the three biodiesel (FAEE1, FAEE2, and FAEE3), except a slight difference noticed in the iodine and acid value of the FAEE1 produced by the BTCPH, this may be attributed to the powder preparation processes. Burning could result in the loss of the volatile nutrient, making the ash more acidic and increase the unsaturation level of the biodiesel when used during the transesterification process (Betiku *et al*., 2017)[11]. The physicochemical properties of the FAEE2 and FAEE3 remain almost the same; this could be attributed to the calcination process involved in the sample preparation, causing the gaseous evolution of CO_2 from the $CaCO_3$ at a controlled temperature more than burning. The properties of biodiesel produced were well within the recommended standard stated by ASTM D6751 [22] and EN 14214[23].

Table 5
Qualities of the produced FAEEs

Parameter	BTO_{60}	FAEEs (%wt.)			ASTM D6751 [22]	EN 14214 [23]
		FAEE1	FAEE2	FAEE3		
Colour@ 27 ^oC	Brownish-yellow	Light yellowish	Light yellowish	Light yellowish	-	-
State @ room temp	Liquid	Liquid	Liquid	Liquid	Liquid	Liquid
Specific gravity	0.902	0.864	0.864	0.864	-	860–900
Viscosity @ 40 ^oC/ (mm^2/s)	22.30	2.78	2.78	2.78	1.9-6.0	3.5-5.0
Moisture content (%)	0.02	< 0.01	< 0.01	< 0.01	< 0.03	0.02
%FFA (as oleic acid)	0.1745	0.032	0.021	0.018	0.40 max	0.25 max
Acid value (mg KOH/g oil)	0.249	0.064	0.042	0.036	0.80 max	0.50 max
Iodine value (g I_2/100 g oil)	58.88	56.62	53.62	53.62	ND	120 max
Saponification value (mg KOH/g oil)	180.00	178.43	176.32	172.22	236.66-253.04	ND
Peroxide value (meq O_2/kg oil)	12.65	8.90	8.70	8.60	ND	12.85
HHV (MJ/kg)	41.17	41.26	41.40	41.52	ND	ND
Cetane number	63.39	64.15	65.19	65.92	57 min	51 min
API gravity	22.30	32.27	32.27	32.27	30–42	ND
Diesel index	49.50	50.26	51.30	52.04	50.4 min	ND
ND = Not Determine						

3.6 Comparative studies of this work with earlier reported works

Table 6 showed the use of single heterogeneous based catalyst derived from different agricultural wastes for biodiesel production using single/blended oil in a different ratio (Subramaniapillai *et al.*, 2019; Fayazishishvan *et al.*, 2018; Tadesse *et al.*, 2019)[8, 27, 28]. Falowo *et al.* (2020)[17] derived a based catalyst from the mixture of three agricultural wastes, while Adepoju *et al.* in their various reported studies, derived novel based catalysts from the mixture of different biomass wastes for biodiesel synthesis. Except the work of Victoria *et al.* (2017) [29], where the authors established the optimum biodiesel yields from Banana fruit peel and Cocoa pod husk, no single report has ever derived three CaO-based catalysts from single biomass waste and compares their efficiencies in fatty acid ethyl ester (FAEE) synthesis. Hence, with respect on earlier reports, there exists no basis, but this study showed that the derived catalysts produced a high yield of biodiesel, and the catalysts can be used in industrial as feedstock.

Table 6
Comparing this study with reported literature studies

Blended oil	Blending ratio (vol/vol)	Catalysts	Calcination temperature and duration	% CaO/KOH conversion	Catalyst analysis	% Biodiesel yield	References
Honne + Rubber seed + Neem oil	20:20:60	Cocoa pod Husk-Plantain peels- kola nut husk	500 °C for 4 h	KOH = 47.67%	XRD, SEM, BET, and FTIR	98.45	Falowo *et al.* (2020)[17]
Pig fat + Neem oil	60:40	*Mixture of* Palm kernel shell husk- Fermented kola nut pod husk	800 °C for 3 h	CaO = 71.20%	EDS, SEM, BET, and FTIR	98.05	Adepoju, (2020) [11]
Cucurbita pepo + *Chrysophyllum albidum* + *papaya oil*	33:33:34	*Mixture of Citrullus lanatus - Musa acuminate* peels	700 ^{o}C for 4 h	CaO = 78.74%	XRD, SEM, BET and FTIR	93.45	Adepoju *et al.* (2020a)[21]
Irvingia gabonensis + *Pentaclethra macrophylla* + *Elais guineensis oil*	33:33:34	*Mixture of* Wood ash-Snail shell- eggshell	900 ^{o}C for 3 h	CaO = 98.50%	SEM, EDX-ray, FTIR and BET	97.22	Adepoju *et al.* (2020b)[24]
Calophyllum inophyllum-waste cooking oil	50:50	Donax deltoids shells	105 °C for 24 h	CaO = 70.87%	XRD, SEM, BET, and FTIR	96.50	Subramaniapillai *et al.* (2019)[8]
Waste cooking oil (WCO)	-	$Ca(NO_3).4H_2O$	500 °C for 5 h	CaO	XRD and SEM	96.00	Tadesse *et al.* (2019)[28]
Sunflower oil	-	Chicken eggshells	900 ^{o}C for 3 h	CaO	SEM, TGA, XRD	83.20%	Fayazishishvan *et al.* (2018)[27]
Palm Kernel oil	-	Banana fruit peel Cocoa pod husk	650 ^{o}C for 4 h	CaO		99.50% 99.30%S	Victoria *et al.* (2017)[29]
Carica papaya + *Citrus sinesis* + *Hibiscus sabdariffa* + Waste used oil	25:25:25:25	*Mixture of Lattorina littorea*-*Mactra coralline* Shell	900 ^{o}C for 3 h	CaO = 99.02	SEM, EDX, FTIR	99.78%	Adepoju *et al.* (2020c)[25]
Luffa cylindrical + *Datura stramonium* + *Lagenaria siceraria* oil	29:50:21	*Mixture of Cucurbita pepo- Musa acuminate - Citrullus lanatus* peels	650 ^{o}C for 3 h	CaO = 75.65%	SEM, EDX-ray, FTIR, and BET	96.50%	Adepoju *et al.* (2020d)[30]
Beef Tallow blend + Waste used vegetable oil	60:40	*Theobroma cacao* pod husks		CaO	XRD, SEM, BET, and FTIR		**THIS STUDY**
		Burnt	Uncontrolled temperature	68.20%		92.81%	
		Calcined	750 ^{o}C for 4 h	81.46%		93.02%	
		Submerged fermented calcined	750 ^{o}C for 4 h	87.65%		99.64%	

4. Conclusion

The blending ratio of oil 60:40 (BTO_{60}) effectively produced a low oil acid value. Three novel catalysts derived using *Theobroma cacao* pod husks were demonstrated as the potential catalysts for FAEEs production and their efficacy could be attributed to the high percentage of calcium present. A hybrid design established an optimum value of 92.81 (%wt.) for FAEE1, 93.02 (%wt.) for FAEE2, and 99.64 (%wt.) for FAEE3, for transesterification process as the reaction time of 78.58 min, catalyst amount of 3. 37 (wt.%), reaction temperature of 79.23 ^{o}C, and EtOH/OMR of 1:6.66 (vol/vol), respectively. Based on catalyst BET adsorption analysis, the percentage CaO-based obtained from the developed catalysts showed *Theobroma cacao* pod husks could be used as industrial feedstock, and the quality of the FAEEs proved are within the ASTM D-6751 and EN 14214 biodiesel standard specifications.

Declarations

5.1 Availability of data and materials

All data generated or analyzed during this study are included in this published article.

5.2 Competing interests

The authors declare that they have no competing interests.

5.3 Funding

This work receives no fund from University, Private organization, or Government body.

5.4 Authors' contributions

Adepoju T. F: Conceptualization, Methodology, Software, Validation, Formal Analysis, Investigation, Resources, Data Curation, Writing-Original Draft, Supervision.

Ibeh, M. A: Formal Analysis, Investigation, Resources, Data Curation, Provide Financial Support, Methodology, Software

Babatunde, E.O: Methodology, Software, Validation, Formal Analysis, Methodology, Investigation, Resources, Provide Financial Support

Asuquo, A. J: Formal Analysis, Investigation, Resources, Data Curation, Methodology

Eloboka, C: Investigation, Resources, Data Curation, Methodology

5.5 Acknowledgment

Authors acknowledge the effort of Technologists of the Department of Chemical Engineering, Akwa Ibom State University, Nigeria. The effort of Eloboka, C of the School of Chemical and Minerals Engineering, Northwest University, Potchefstroom, South Africa, is also appreciated. Especial thanks to my project students and staff of Chemical Engineering, Akwa Ibom State University, Nigeria.

References

1. N. Dizge, B. Keskinler, A. Tanriseven, Biodiesel production from canola oil by using lipid immobilized onto hydrophobic microporous strene-divinylbenzene copolymer. Biochemic Engineer Journ. 44(2009)220–225.
2. D. K. Milan, V. V. Ana, M. J. Natasa, S. S. Olivera, B.V. Vlada, Optimization and kinetic of esterification of the oil obtained from plum stones as a pre-treatment step in biodiesel production. Waste Managem. 48 (2016) 619–629.
3. V. Vadery, B.N. Narayanan, R.M. Ramakrishnan, S.K. Cherikkallinmel, S. Sugunan, D.P. Narayanan. Room temperature production of jatropha biodiesel over coconut husk ash. Energ. 70 (2014) 588–594.
4. A. Bazargan, M.D. Kostic, O. S. Stamenkovic, V. B. Veljkovic, G. McKaV, Palm kernel shell gasification residues as precursors for a calcium based catalyst for biodiesel production. Fuel, 150 (2015) 519–525.
5. A.P.S. Chouhan, and A.K. Sarma, Biodiesel production from *Jatropha curcus* L. oil using *Lemna perpusila* Torrey ash as heterogeneous catalyst. Biomas. Bioenerg. 55(2013)386–390.
6. R. Rezaei, M. Mohadesi, G. R. Moradi, Optimization of biodiesel production using waste mussel shell catalyst. Fuel, 109(2013)534–541.
7. B. L. Ikbal, R. Kalyani, G. Rajat, C. Sushovan, P. Bappi, R. Laithazuala, Waste snail shell derived heterogeneous catalyst for biodiesel production by the transesterification of soybean oil. RSC Adv. 8 (2018) 20131. Doi: 10.1039/c8ra02397b
8. N. Subramaniapillai, V. Govindaraj, B. Muthusamy. Process optimization of *Calophyllum inophyllum*-waste cooking oil mixture for biodiesel production using Donax deltoids shells as Heterogeneous catalyst. Sustain Environ Res. 29 (2019) 2351–2362. https://doi.org/10.1186/s42834-019-0015-6.
9. Adepoju, T. F., Rasheed, B., Olatunji, M.O., Ibeh, M.A., Ademiluyi, F.T., Olatunnbosun, B. E. 2018. Modeling and optimization of lucky nut seed by pearl spar catalysed transesterification. *Heliyon*, 4 e00798, doi: 10.1016j.
10. E. Betiku, and S.O. Ajala, Modelling and Optimization of *Thevetia peruviana* (yellow oleander) oil biodiesel synthesis via *Musa paradisiacal* (plantain peels) as heterogeneous catalyst: a case of artificial neural network vs. response surface methodology. Ind Crops Prod. 53 (2015) 314–322.
11. E. Betiku, A. O. Etim, O. Pereore, T. V. Ojumu, Two-step conversion of neem seed (*Azadirachta indica*) oil into fatty methyl esters using a bio-base catalyst: An example of cocoa pod husk. *Energ & Fuels 31* (2017) 6182–6193 (America Chemical Society)
12. B. Nath, B. Das, P. Kalita, S. Basumatary, Waste to value addition: Utilization of waste Brassica nigra plant derived novel green heterogeneous base catalyst for effective synthesis of biodiesel. *J. of Clean Prod.* 239 (2019) 118112.
13. M. Balajii and S. Niju, Banana peduncle–A green and renewable heterogeneous base catalyst for biodiesel production from Ceiba pentandra oil. *Renew Energ*, 146 (2020) 2255–2269.
14. G. Minakshi, L. Khairujjaman, K. P. Atanu, D. Niran, M. Mrutyunjay, K. G. Imon, H. Anil, B. Utpal, D. Dhanapati, Carica papaya stem: A source of versatile heterogeneous catalyst for biodiesel production and CeC bond formation. Renew. Energ. 147 (2020) 541–555.
15. H. Hadiyanto, P. L. Sri, W. Widayat, Preparation and Characterization of *Anadara Granosa* Shells and $CaCO_3$ as Heterogeneous Catalyst for Biodiesel Production. BCREC. 11 (2016) 21–26.
16. S. Trisupakitti, C. Ketwong, W. Senajuk, C. Phukapak, C. Wiriyaumpaiwong, Golden Apple Cherry Snail Shell as Catalyst for Heterogeneous Transesterification of Biodiesel. Brazilian J Chem Eng. 35 (2019) 1283–1291

17. O. A. Falowo, P. Omoniyi, T.V. Ojumu, E. Betiku, Sustainable biodiesel synthesis from Honne-Rubber-Neem oil blend with a novel mesoporous base catalyst synthesis from a mixture of three agrowastes, Cataly. 10 (2020) 1–24.
18. Adepoju, T. F. **Optimization processes of biodiesel production from pig and Neem (Azadirachta indica A.Juss) seeds blend oil using alternative catalysts from waste biomass**. Ind Crops Prod. 149 (2020) 112334.
19. **AOAC. Official methods of analyses of the Association of Official Analytical Chemists**. 1990
20. **AOAC. Official methods of analyses of the Association of Official Analytical Chemists**. 1997
21. T. F., Adepoju, M.A. Ibeh, E. O., Babatunde, A. J. Asuquo, Methanolysis of CaO based catalyst derived from egg shell-snail shell-wood ash mixed for fatty acid methylester (FAME) synthesis from a ternary mixture of *Irvingia gabonensis -Pentaclethra macrophylla - Elais guineensis* oil blend: An application of simplex lattice and central composite design optimization. Fuel. 275 (2020a) 117997.
22. ASTM D6751. Standard Test Method for Gross Calorific Value of Oil, Water, Coal and Coke by the adiabatic Bomb Calorimeter from SAI Global.
23. EN 14214. European Committee for Standardization, describing the requirements and test methods for FAME.
24. T. F. Adepoju, M. A. Ibeh, E. O. Babatunde, A. J. Asuquo, Biodiesel Production from Underutilized Oil-Seed via a Solid Based Catalyst Synthesized from the Mixture of three Agricultural Waste Peels. BAB_2020b_453 (Accepted)
25. T. F. Adepoju, M. A. Ibeh, U. Ekanem, A. J. Asuquo, Data on the derived mesoporous based catalyst for the synthesized of fatty acid methyl ester (FAME) from ternary oil blend: An optimization approach. Data in Brief 30 (2020) 105514
26. C. G. Arjun, M. G. Jounnever, J. A. Meljane, S. V. Rohoney, R-L. Jay. Laranang, F.M. Val Irvin, O.A. Renato, L. I. Alexander, Response surface optimization of biodiesel yield from pre-treated waste oil of rendered pork from a food processing industry. Bioresourc and Bioprocess, 6 (2019) 48. https//:10.1186/s40643-019-02842.
27. E. Fayazishishvan, B. Ghobadian, H. K. Van de Bovenkamp, G. Najafi, B. Hosseinzadehsamani, H. J. Heeras, J. Yuen, Optimization of Biodiesel Production over Chicken Eggshell-Derived CaO Catalyst in a Continuous Centrifugal Contractor Separator. IECR. 57(2018)12742–12755. https://doi.org/10.1021/acs.iecr.8b02678.
28. A. D. Tadesse, T. M. Tadios, S. M. Yedilfan, Optimized Biodiesel Production from Waste Cooking Oil (WCO) using Calcium oxide (CaO) Nano-catalyst. Scientif Reports, 9(2019)18982. https://doi.org/10.1038/s41598-019-55403-4.
29. O. O. Victoria, J. A. Ayo, O. O. Oluwaseyi, O. A. Omowumi, B. I. Niyi, O. E. Anietie, B. Eriola, Application of Agricultural Waste-Based Catalysts to Transesterification of Esterified Palm Kernel Oil Biodiesel: A case of Banana Fruit Peel Versus Cocoa Pod Husk. Wast Biomas Valoriza, (2017) https://doi.org/10.1007/s12649-017-0152-2
30. T. F. Adepoju, M. A. Ibeh, E. N. Udoetuk, A. J. Asuquo, E. O. Babatunde, Quaternary blend of *Carica papaya - Citrus sinesis - Hibiscus sabdariffa* - Waste used oil for biodiesel synthesis using CaO-based catalyst derived from binary mix of *Lattorina littorea* and *Mactra coralline* Shell. RENE-D-2020d-00352. (Accepted)

Figures

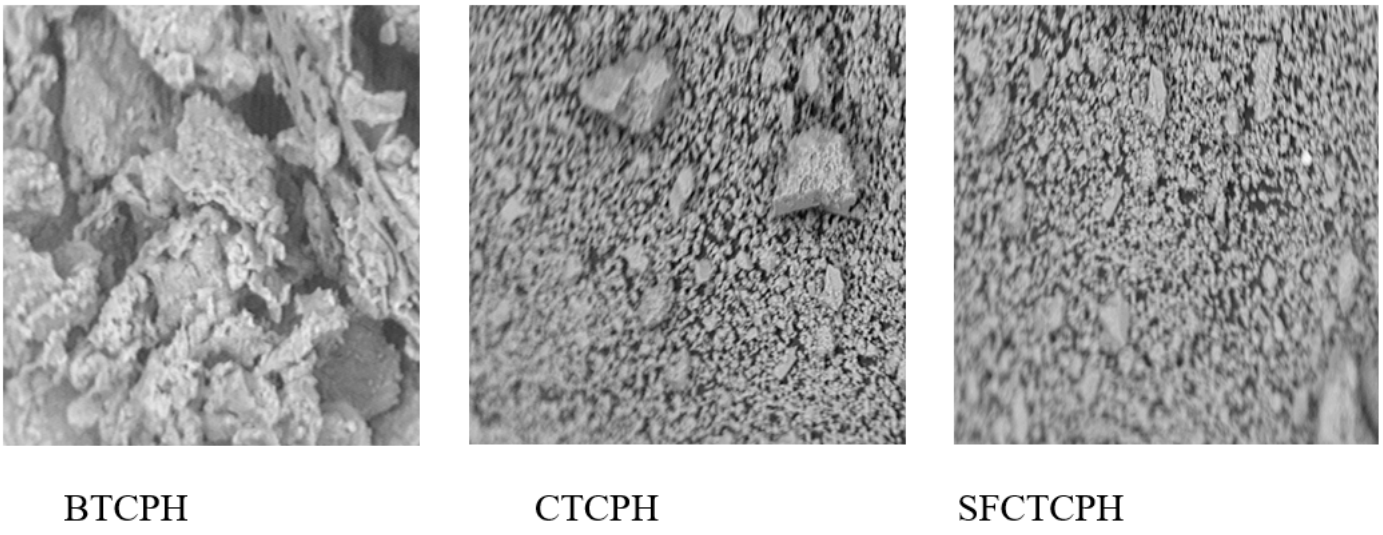

Figure 1

(a-c): SEM images of calcined catalysts

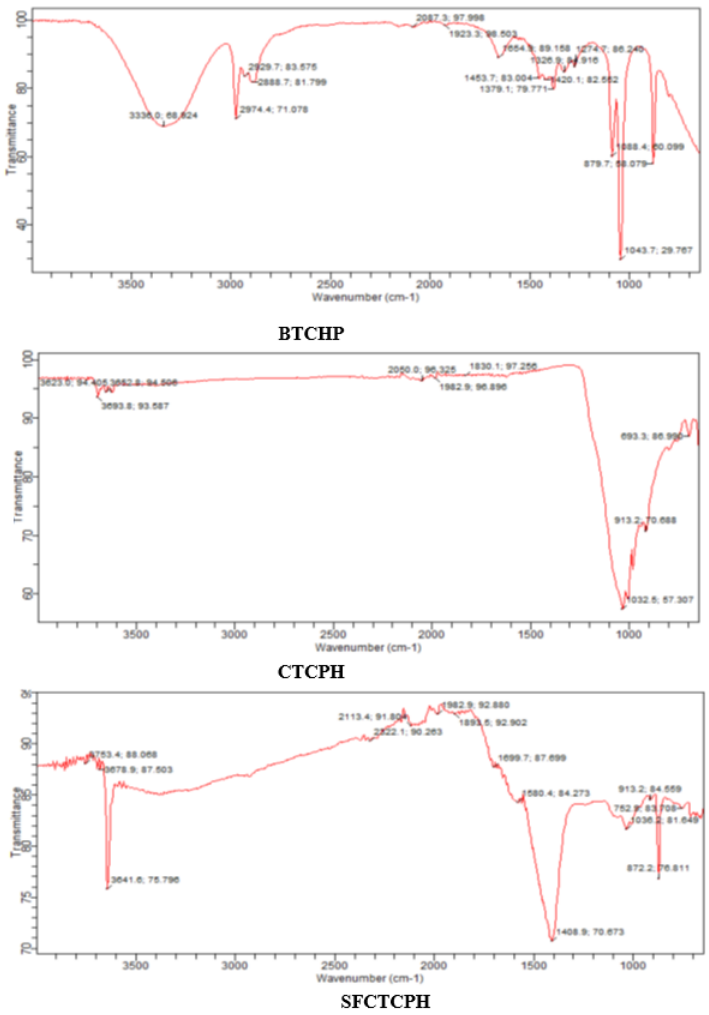

Figure 2

FTIR spectral analysis of the catalysts and the mixed catalyst

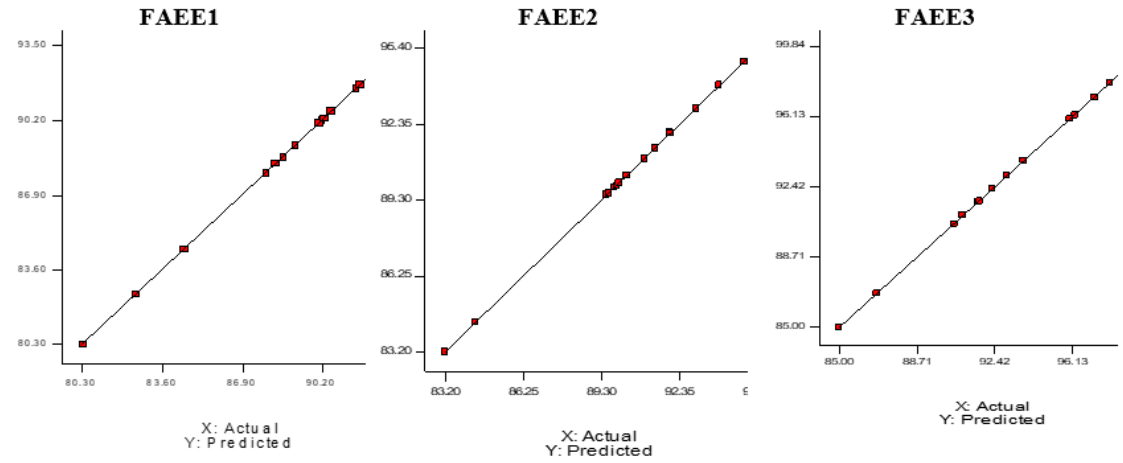

Fig. 2a: Predicted against Actual

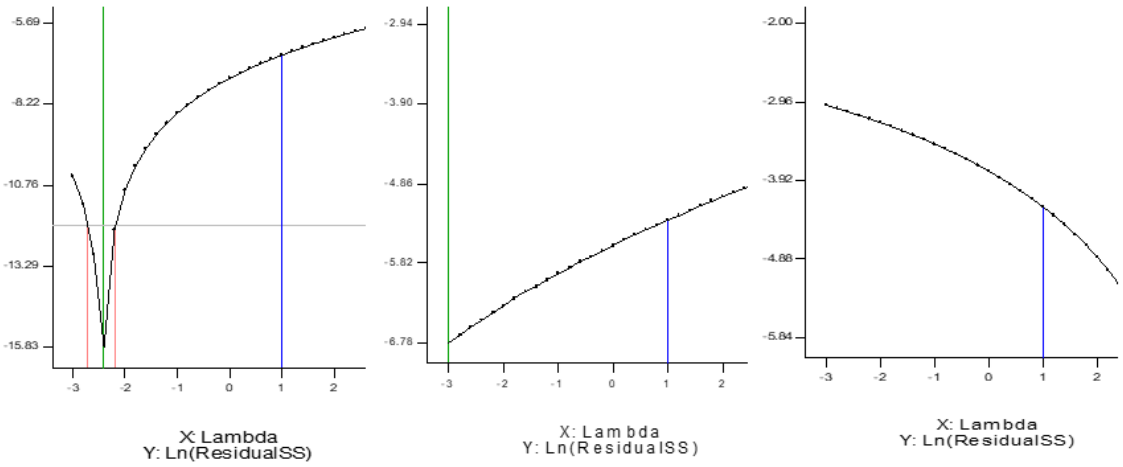

Figure 3

a: Predicted against Actual. b: Box-Cox Plot for Power Transformation

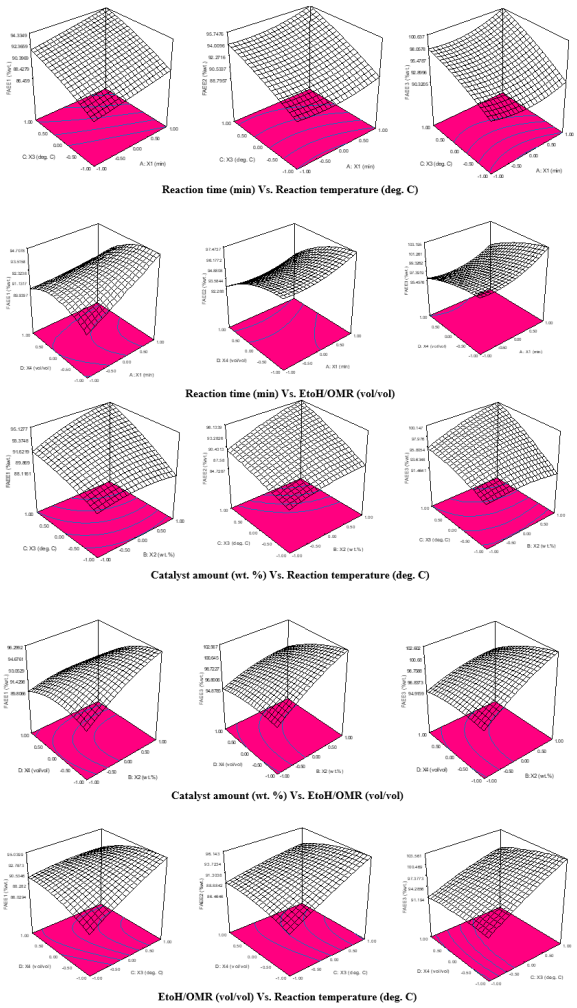

Figure 4

Three-dimensional contour plots showing the interaction of variables on the responses while keeping other factors constant

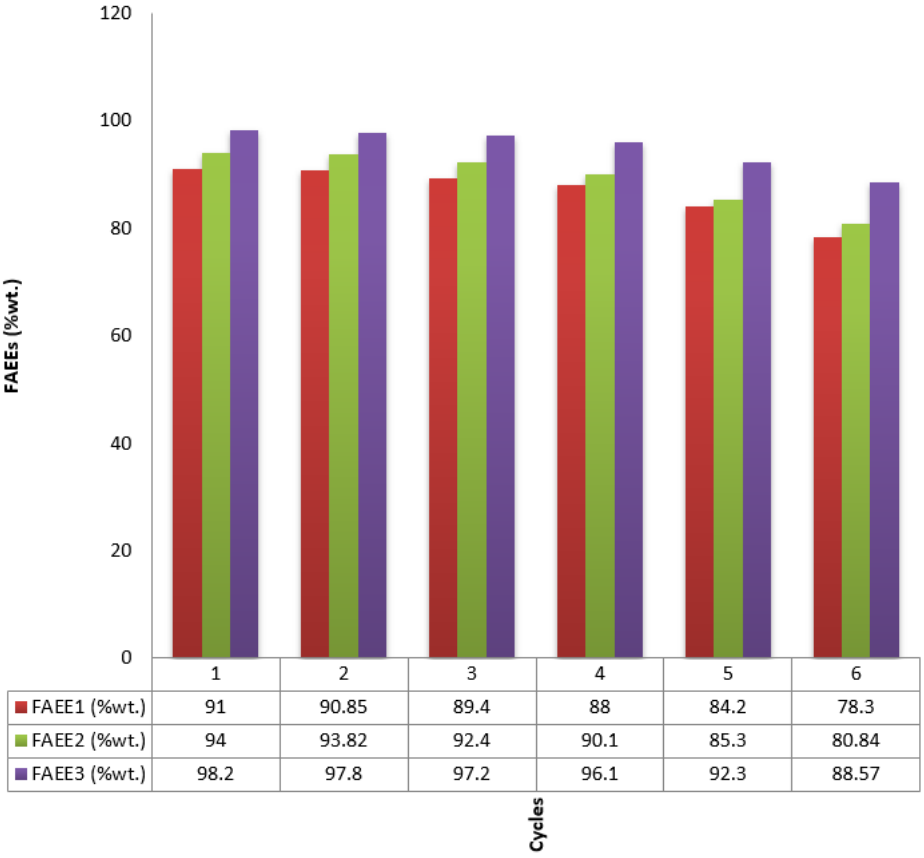

	1	2	3	4	5	6
FAEE1 (%wt.)	91	90.85	89.4	88	84.2	78.3
FAEE2 (%wt.)	94	93.82	92.4	90.1	85.3	80.84
FAEE3 (%wt.)	98.2	97.8	97.2	96.1	92.3	88.57

Figure 5

Plots of results of catalysts reusability test

Supplementary Files

This is a list of supplementary files associated with this preprint. Click to download.

- GraphicalAbstract.docx